



## DNA strand cleaving properties and hypoxia-selective cytotoxicity of 7-chloro-2-thienylcarbonyl-3-trifluoromethylquinoxaline 1,4-dioxide

Venkatraman Junnotula<sup>a</sup>, Anuruddha Rajapakse<sup>a</sup>, Leire Arbillaga<sup>b</sup>, Adela López de Cerain<sup>b</sup>, Beatriz Solano<sup>c</sup>, Raquel Villar<sup>c</sup>, Antonio Monge<sup>c</sup>, Kent S. Gates<sup>a,\*</sup>

<sup>a</sup> Departments of Chemistry and Biochemistry, University of Missouri-Columbia, Columbia, MO 65211, USA

<sup>b</sup> Laboratorio de Toxicología, Centro de Investigación en Farmacobiología, Aplicada (CIFA), University of Navarra, C/Irunlarrea 1, 31080 Pamplona, Spain

<sup>c</sup> Unidad de Investigación y Desarrollo de Medicamentos, Centro de Investigación en Farmacobiología Aplicada (CIFA), University of Navarra, C/Irunlarrea 1, 31080 Pamplona, Spain

### ARTICLE INFO

#### Article history:

Received 16 February 2010

Revised 15 March 2010

Accepted 16 March 2010

Available online 19 March 2010

#### Keywords:

Tumor hypoxia

Antitumor agent

DNA-damaging agent

### ABSTRACT

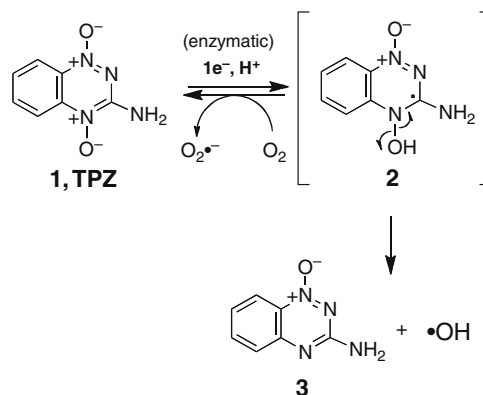
The heterocyclic N-oxide, 3-amino-1,2,4-benzotriazine 1,4-dioxide (tirapazamine, **1**), shows promising antitumor activity in preclinical studies, but there is a continuing need to explore new compounds in this general structural category. In the work described here, we examined the properties of 7-chloro-2-thienylcarbonyl-3-trifluoromethylquinoxaline 1,4-dioxide (**9h**). We find that **9h** causes redox-activated, hypoxia-selective DNA cleavage that mirrors the lead compound, tirapazamine, in both mechanism and potency. Furthermore, we find that **9h** displays hypoxia-selective cytotoxicity against human cancer cell lines.

© 2010 Elsevier Ltd. All rights reserved.

### 1. Introduction

It is well established that solid tumors contain substantial regions that are low in oxygen (hypoxic).<sup>1,2</sup> This property may be exploited in the development of drugs that selectively kill tumor cells.<sup>3–7</sup> Heterocyclic N-oxides are an important class of hypoxia-selective antitumor agents that is exemplified by the lead compound 3-amino-1,2,4-benzotriazine 1,4-dioxide (tirapazamine, **1**, Scheme 1).<sup>4,8–11</sup> Tirapazamine's promising medicinal properties stem from its ability to cause lethal DNA damage in hypoxic tumor cells.<sup>12–18</sup> Tirapazamine-induced DNA damage is initiated by intracellular enzymatic one-electron reduction of the drug.<sup>9,12,13,19–23</sup> In normal aerobic cells, the resulting radical **2** undergoes back-oxidation to regenerate the parent drug and superoxide radical (Scheme 1).<sup>8,9,12,13,19–22</sup> This type of redox cycling can be cytotoxic;<sup>6</sup> however, in the context of tirapazamine, reactions of the drug radical **2** in the absence of molecular oxygen evidently are more lethal.<sup>9,12,13,22</sup> Under hypoxic conditions, the drug radical decomposes to release either the well known DNA-damaging cytotoxin, hydroxyl radical<sup>21,24–27</sup> or a highly reactive benzotriazinyl radical **4**.<sup>28–31</sup> The antitumor activity of tirapazamine has been examined in many phase I, II, and III clinical trials over the past 15 years, but the compound has not been approved for clinical use.<sup>32,33</sup> Thus, there is a continuing need to explore new compounds in this general structural category.

A number of heterocyclic N-oxides display properties analogous to tirapazamine. For example, various 1,2,4-benzotriazines,<sup>34–40</sup> quinoxaline 1,4-di-N-oxides (e.g., **5**),<sup>41–47</sup> phenazine 5,10-di-N-oxides (**6**),<sup>48–51</sup> and imidazo[1,2-*a*]quinoxaline N-oxides (**7**)<sup>52</sup> exhibit hypoxia-selective cytotoxicity in preclinical tests. In some cases, the compounds also have been shown to display hypoxia-selective DNA-damaging properties analogous to tirapazamine.<sup>41,42</sup> Toward the goal of identifying new, clinically useful agents, it is important to examine the properties of structurally varied heterocyclic N-oxides. Along these lines, Solano et al. recently prepared and



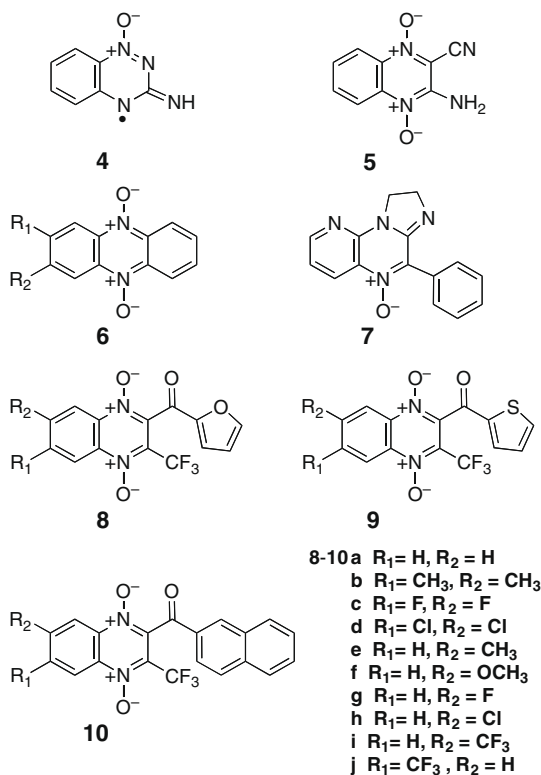
Scheme 1. Bioactivation of tirapazamine (**1**).

\* Corresponding author. Tel.: +1 573 882 6763; fax: +1 573 882 2754.

E-mail address: [gatesk@missouri.edu](mailto:gatesk@missouri.edu) (K.S. Gates).

characterized a series of substituted quinoxaline di-N-oxides **8–10**.<sup>43</sup> These analogues show potent activity against human cancer cell lines in aerobic cell culture (LC<sub>50</sub> values 2–10  $\mu$ M) and it was suggested that the redox-cycling abilities of these compounds might contribute to their potent aerobic cytotoxicity.<sup>43</sup> Importantly, **9c** and **9h** also showed promising in vivo activity in hollow fiber tumor model studies.<sup>43</sup>

Given the structural similarity of these compounds to the hypoxia-selective antitumor agent tirapazamine and their in vivo activity in hollow fiber models where hypoxia could play a role in bioactivity<sup>53,54</sup> we felt it would be informative to examine the ability of these compounds to carry out redox-activated DNA strand cleavage under hypoxic conditions. We find that **9h** causes redox-activated, hypoxia-selective DNA cleavage that mirrors the lead compound, tirapazamine, in both mechanism and potency. Furthermore, we find that **9h** displays hypoxia-selective cytotoxicity against human cancer cell lines. The hypoxic cytotoxicity ratio (HCR) for **9h** is 16 whereas that for tirapazamine is 75. The lower HCR for **9h** may arise, at least in part, because this compound undergoes more efficient aerobic redox cycling than tirapazamine.



## 2. Results and discussion

### 2.1. Redox-activated, hypoxia-selective DNA strand cleavage by 7-chloro-2-thienylcarbonyl-3-trifluoromethyl quinoxaline 1,4-dioxide (**9h**)

Compound **9h** was synthesized as described previously.<sup>43</sup> We used NADPH:cytochrome P450 reductase to carry out one-electron reductive activation of **9h**. This type of reductase is thought to be primarily responsible for in vivo activation of TPZ.<sup>20,59,60</sup> Molecular oxygen was removed from stock solutions by three cycles of freeze-pump-thaw degassing and the assays assembled and incubated in an inert atmosphere glove bag. We first examined the

potential of **9h** to cut double-stranded, supercoiled plasmid DNA. In this assay, single-strand cleavage converts supercoiled plasmid DNA (form I) to the open-circular form (form II).<sup>61–63</sup> The two forms of plasmid DNA are then separated using agarose gel electrophoresis, the gel stained with a DNA-binding dye such as ethidium bromide, and the relative amounts of cut and uncut plasmid quantitatively determined by digital image analysis. The direct strand breaks (not requiring thermal or basic workup) monitored in this type of experiment typically arise via the reaction of radicals with hydrogen atoms on 2'-deoxyribose residues in the backbone of DNA.<sup>64–70</sup> The possibility of background DNA damage resulting from enzymatic reduction of traces of molecular oxygen to superoxide was suppressed by addition of desferal to sequester adventitious trace metals in a non-redox active form. This prevents the conversion of superoxide-derived hydrogen peroxide to hydroxyl radical.<sup>71</sup> As a further precaution, the assays contained superoxide dismutase and catalase to decompose any superoxide radical and hydrogen peroxide that was produced.<sup>71</sup> DNA-cleavage assays reported here were conducted using N-oxide concentrations between 1 and 25  $\mu$ M.

We find that **9h** caused DNA strand cleavage when incubated with the NADPH:cytochrome P450 enzyme system under hypoxic conditions (Fig. 1). The yields of DNA cleavage by **9h** were somewhat higher than tirapazamine (Fig. 2). Control experiments showed that strand cleavage was abrogated if enzyme, NADPH, or **9h** were omitted from the reaction mixtures. Likewise, no significant DNA cleavage occurred under aerobic conditions. Addition of classical radical scavenging agents<sup>71</sup> such as methanol, ethanol, *t*-butanol, DMSO, and mannitol (500 mM) substantially suppressed strand cleavage (70–80% inhibition, Fig. 3).

Overall, the data suggests that one-electron enzymatic reduction of **9h** yields an oxygen-sensitive radical intermediate that leads to DNA strand cleavage selectively under hypoxic conditions.

The xanthine/xanthine oxidase enzyme system has been used to initiate DNA strand cleavage by tirapazamine and quinoxaline 1,4-dioxide.<sup>19,21,42</sup> We found that the xanthine/xanthine oxidase enzyme system similarly activated DNA strand cleavage by **9h** under hypoxic conditions (Fig. 4). Interestingly, the behavior of **9h** with the xanthine/xanthine oxidase enzyme system is different from that of 3-amino-2-quinoxalinecarbonitrile 1,4-dioxide (**5**), a quinoxaline derivative that displays hypoxia selective cytotoxicity comparable to tirapazamine.<sup>44,45</sup> Compound **5** undergoes two-electron reduction by xanthine/xanthine oxidase *without* the release of an intermediate oxygen-sensitive, DNA-damaging radical.<sup>41</sup> In contrast, it seems that injection of a second electron into the radical anion **11** (Scheme 2) derived from **9h** is not within the reducing power of the xanthine/xanthine oxidase system.

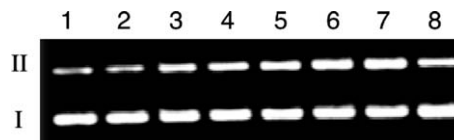


**Figure 1.** DNA cleavage by various concentrations of reductively activated **9h** under anaerobic conditions. Supercoiled plasmid DNA (33  $\mu$ g/mL, pGL-2 Basic) was incubated with **9h** (5–25  $\mu$ M), NADPH (500  $\mu$ M), cytochrome P450 reductase (33 mU/mL), catalase (100  $\mu$ g/mL), superoxide dismutase (10  $\mu$ g/mL), sodium phosphate buffer (50 mM, pH 7.0), acetonitrile (0.5–2.5% v/v), and desferal (1 mM) under anaerobic conditions at room temperature for 16 h, followed by agarose gel electrophoretic analysis. Lane 1, DNA alone ( $S = 0.25 \pm 0.04$ ); lane 2, NADPH (500  $\mu$ M) + reductase (33 mU/mL) ( $S = 0.25 \pm 0.04$ ); lanes 3–7, NADPH (500  $\mu$ M) + reductase (33 mU/mL) + **9h** (5  $\mu$ M, lane 3) ( $S = 0.37 \pm 0.05$ ); (10  $\mu$ M, lane 4) ( $S = 0.43 \pm 0.05$ ); (15  $\mu$ M, lane 5) ( $S = 0.52 \pm 0.03$ ); (20  $\mu$ M, lane 6) ( $S = 0.58 \pm 0.02$ ); (25  $\mu$ M, lane 7) ( $S = 0.68 \pm 0.04$ ); lane 8, **9h** (25  $\mu$ M) ( $S = 0.26 \pm 0.05$ ). The values,  $S$ , derived from agarose gel data and represent the mean number of strand breaks per plasmid molecule and were calculated using the equation  $S = -\ln f_1$ , where  $f_1$  is the fraction of plasmid present as form I.

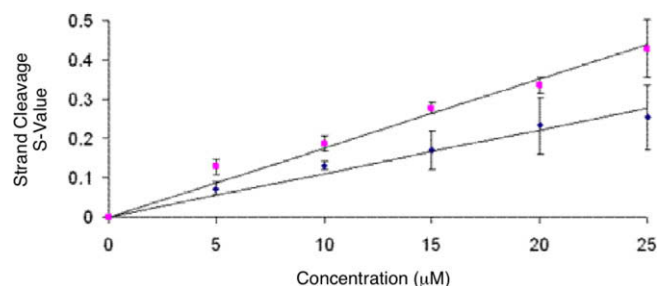


**Figure 2.** Comparison of DNA cleavage by reductively activated **9h** and tirapazamine under anaerobic conditions (upper line represents strand cleavage by **9h**, while the lower line is that by tirapazamine. Supercoiled plasmid DNA (33 μg/mL, pGL-2 Basic) was incubated with **9h** or TPZ (5–25 μM), NADPH (500 μM), cytochrome P450 reductase (33 mU/mL), catalase (100 μg/mL), superoxide dismutase (10 μg/mL), sodium phosphate buffer (50 mM, pH 7.0), acetonitrile (0.5–2.5% v/v), and desferal (1 mM) under anaerobic conditions at room temperature for 16 h, followed by agarose gel electrophoretic analysis. The values,  $S$ , derived from agarose gel data and represent the mean number of strand breaks per plasmid molecule and were calculated using the equation  $S = -\ln f_i$ , where  $f_i$  is the fraction of plasmid present as form I. Background cleavage in the untreated plasmid was subtracted to allow direct comparison of DNA cleavage yields between different experiments.

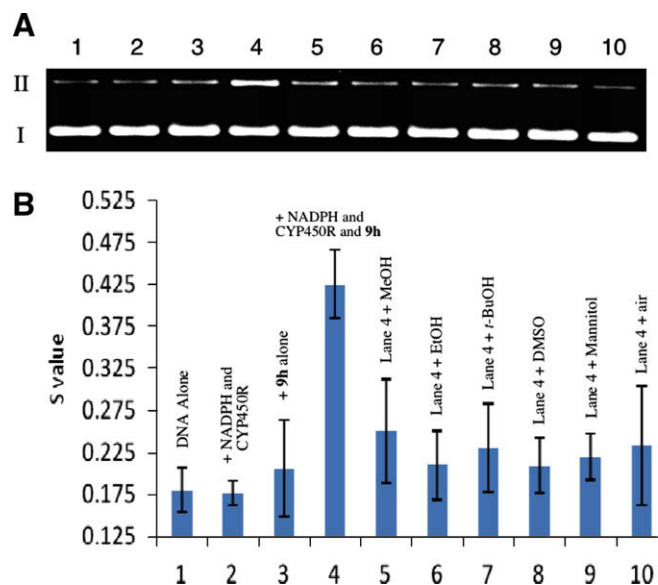


**Figure 3.** Effects of various additives on the cleavage of supercoiled plasmid DNA by **9h** (25 μM) in the presence of NADPH (500 μM) and cytochrome P450 reductase (33 mU/mL) as an activating system. All reactions contained DNA (33 μg/mL, pGL-2 Basic), sodium phosphate buffer (50 mM, pH 7.0), acetonitrile (2.5% v/v), catalase (100 μg/mL), superoxide dismutase (10 μg/mL), and desferal (1 mM) and were incubated under anaerobic conditions (except lane 10) at 24 °C for 16 h, followed by agarose gel electrophoretic analysis. Lane 1, DNA alone ( $S = 0.18 \pm 0.02$ ); lane 2, NADPH (500 μM) + reductase (33 mU/mL) ( $S = 0.18 \pm 0.01$ ); lane 3, **9h** (25 μM) + DNA ( $S = 0.20 \pm 0.06$ ); lane 4, **9h** (25 μM) + NADPH (500 μM) + reductase (33 mU/mL) ( $S = 0.43 \pm 0.04$ ); lanes 5–9, **9h** (25 μM) + NADPH (500 μM) + reductase (33 mU/mL) + methanol (500 mM, lane 5) ( $S = 0.25 \pm 0.06$ ); ethanol (500 mM, lane 6) ( $S = 0.21 \pm 0.04$ ); *tert*-butyl alcohol (500 mM, lane 7) ( $S = 0.23 \pm 0.05$ ); DMSO (500 mM, lane 8) ( $S = 0.21 \pm 0.03$ ); mannitol (500 mM, lane 9) ( $S = 0.22 \pm 0.03$ ); lane 10, **9h** (25 μM) + NADPH (500 μM) + reductase (1 mU) + air ( $S = 0.23 \pm 0.07$ ). In Panel A, a representative gel is shown. In Panel B, the yields of strand cleavage for various reaction conditions are shown. The value  $S$  represents the mean number of strand breaks per plasmid molecule and is calculated using the equation  $S = -\ln f_i$ , where  $f_i$  is the fraction of plasmid present as form I.

## 2.2. NADPH:cytochrome P450 reductase-catalyzed metabolism of **9h**

As shown in Scheme 1, in vitro hypoxic one-electron bioreductive activation of tirapazamine by enzyme systems such as

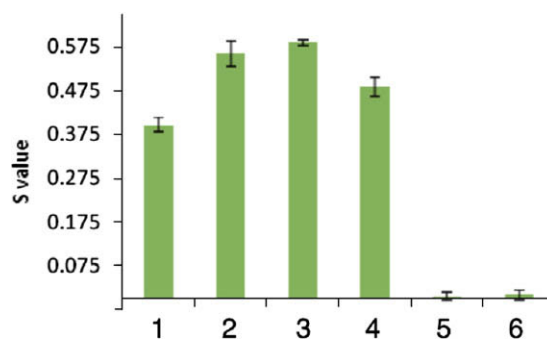
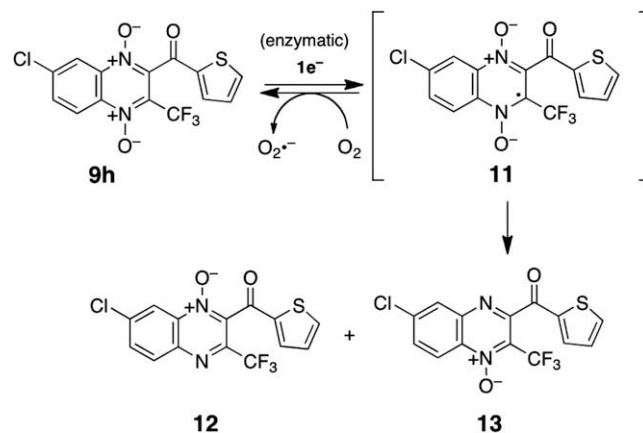


**Figure 4.** Comparison of reductive activation of **9h** and tirapazamine by xanthine/xanthine oxidase and NADPH:cytochrome P450 reductase enzyme systems. Supercoiled plasmid DNA (33 μg/mL, pGL-2 Basic) was incubated with **9h** or tirapazamine (20 μM) and either xanthine (500 μM) and xanthine oxidase (12 mU) or NADPH (500 μM) and cytochrome P450 reductase (33 mU/mL), along with catalase (100 μg/mL), superoxide dismutase (10 μg/mL), sodium phosphate buffer (50 mM, pH 7.0), containing 2.0% acetonitrile v/v, and desferal (1 mM) under anaerobic conditions at room temperature for 16 h, followed by agarose gel electrophoretic analysis. Reaction lanes: 1, **9h** with xanthine and xanthine oxidase; lane 2, **9h** with NADPH and cytochrome P450 reductase; lane 3, tirapazamine with xanthine and xanthine oxidase; lane 4, tirapazamine with NADPH and cytochrome P450 reductase; lane 5, xanthine and xanthine oxidase alone; lane 6, NADPH and cytochrome P450 reductase alone. The value,  $S$ , derived from agarose gel data represents the mean number of strand breaks per plasmid molecule and was calculated using the equation  $S = -\ln f_i$ , where  $f_i$  is the fraction of plasmid present as form I. The  $S$  value of untreated plasmid was subtracted from  $S$  value measured for each reaction.



**Scheme 2.** Bioactivation of compound **9h**.

NADPH:cytochrome P450 reductase or xanthine/xanthine oxidase produces 3-amino-1,2,4-benzotriazine-1-oxide **3**<sup>19,56,72</sup> alongside small amounts of 3-amino-1,2,4-benzotriazine (**14**) and 3-amino-1,2,4-benzotriazine 4-oxide (**15**).<sup>12,19,56,72,73</sup> Other 1,2,4-benzotriazine and quinoxaline 1,4-di-N-oxides generate an analogous set of metabolites.<sup>24,41,42,56</sup> To examine whether the metabolism of **9h** parallels that of tirapazamine we examined the products generated by one-electron reductive activation of **9h** by NADPH:cytochrome P450 reductase under anaerobic conditions.

Reverse-phase HPLC analysis of the products resulting from enzymatic activation of **9h** under hypoxic conditions revealed three major products eluting between 23 and 25 min (Fig. 5). The products displaying retention times of 23 and 24.6 min co-eluted with authentic standards of 7-chloro-2-thienylcarbonyl-3-trifluoromethyl quinoxaline 1-oxide (**12**) and 7-chloro-2-thienylcarbonyl-3-trifluoromethyl quinoxaline 4-oxide (**13**), respectively.

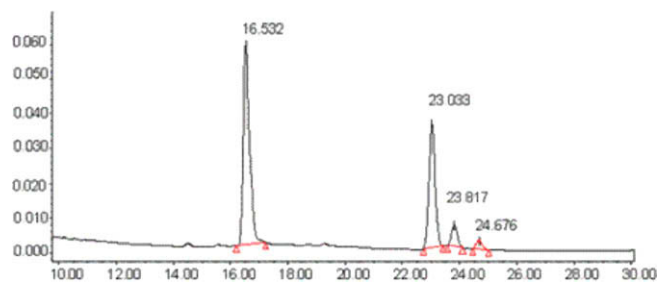
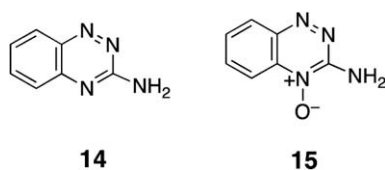


**Figure 5.** HPLC chromatogram of products arising from in vitro metabolism of **9h** by NADPH:cytochrome P450 reductase under anaerobic conditions. Compound **9h** (200  $\mu$ M) was incubated with NADPH:cytochrome P450 reductase (330 mU/mL) and NADPH (500  $\mu$ M) in sodium phosphate buffer (pH 7.0, 50 mM), acetonitrile (20% v/v) containing desferal (1 mM) for 16 h, under anaerobic conditions. The resulting mixture was analyzed by reverse phase HPLC as described in Section 4.



The metabolites were further analyzed using LC/ESI-MS. The mono-N-oxides **12** and **13** were expected to display strong  $[M+H]^+$  ions at  $m/z$  359 along with prominent  $[M+2+H]^+$  signals at  $m/z$  361 due to the significant natural abundance of the  $^{37}\text{Cl}$  isotope. Figure 6A shows the selected ion chromatogram obtained by monitoring these masses. We found that all three of the compounds observed between 23 and 25 min using UV–vis detection display masses consistent with mono-N-oxide derivatives. Again, the retention times of the early and late eluting peaks in this trio of metabolites correspond to **12** and **13**, respectively. Data from both UV-absorption and ion current detection methods suggest that **12** is the major metabolite (Figs. 5 and 6A). The mechanistic basis for the predominant formation of metabolite **12** remains unclear at this time. The compound with intermediate retention time (24 min) has the same mass observed for the  $[M+H]^+$  ion of **12** and **13** and displays a mass spectrum nearly identical to **12** (Fig. 6B). The presence of this third metabolite is intriguing but the structure of this compound remains uncertain at this time. LC/MS/MS analysis of the compound eluting at 23 min showed that the parent ions at  $m/z$  358 and 360 fragment with a loss of 84 mass units, consistent with ejection of the thienyl fragment (Fig. 6B). In addition, an ion resulting from loss of both the thienylcarbonyl and oxide fragments is observed. In contrast, the 4-oxide **13** shows an ion resulting from loss of 84 mass units as the only major fragment ion, followed by less intense signals for sequential losses of CO (–28 mass units) and the oxide fragment (–16 mass units, Fig. 6C).

The mono-N-oxides **12** and **13** (Scheme 2), generated by NADPH:cytochrome P450 reductase-catalyzed metabolism of **9h** did not cause detectable DNA damage either alone or in the presence of the enzymatic reducing system under anaerobic conditions (Fig. 3).

### 2.3. Oxidation of DMSO to methanesulfinic acid by reductively-activated **9h** under hypoxic conditions

Our previous work provided evidence that 1,2,4-benzotriazine 1,4-dioxides release the well known DNA-damaging agent hydroxyl radical, or a similarly reactive diffusible oxidant, following one-electron reductive activation under hypoxic conditions.<sup>21,24–27</sup>

To further explore the mechanism of DNA strand cleavage caused by **9h**, we carried out enzymatic activation of this compound in the presence of the hydroxyl radical trapping agent dimethyl sulfoxide (DMSO). It is well established that reaction of hydroxyl radical with DMSO yields methanesulfinic acid **16** as a characteristic product.<sup>58,74,75</sup> Methanesulfinic acid (**16**) produced in these reactions is often quantitatively detected as the methane diazosulfone **18** following derivatization with the diazonium salt **17** (Scheme 3).<sup>58,74,76</sup>

In our case, treatment of **9h** with NADPH:cytochrome P450 reductase under anaerobic conditions in the presence of DMSO, followed by treatment with **17**, produced a 50% yield of the methanesulfinic acid derivative **18** (based on **9h**). The reported yield was corrected for small amounts of methanesulfinic acid produced during incubation of DMSO with **9h** alone or with the NADPH:cytochrome P450 reductase enzyme system. Overall, the results suggest that **9h** generates substantial yields of hydroxyl radical, or a similarly reactive oxidant, following bioreductive activation.

### 2.4. Hypoxia-selective cytotoxicity of **9h** against V79 cells

Given that compound **9h** displays hypoxia-selective DNA-cleaving properties comparable to the anticancer drug candidate tirapazamine, we felt it was important to examine the hypoxia-selective cytotoxicity of this new compound against mammalian cell lines. We employed a clonogenic assay to characterize the cytotoxicity of **9h** toward V79 Chinese hamster lung fibroblasts under aerobic and anaerobic conditions. Compound **9h** produced 99% cell kill at 2.5  $\mu$ M and 0.21  $\mu$ M under aerobic and anaerobic conditions, respectively. By way of comparison, tirapazamine gave 99% cell kill at 30  $\mu$ M and 2.0  $\mu$ M under aerobic and anaerobic conditions, respectively. It is clear that **9h** is more cytotoxic than tirapazamine under both hypoxic and aerobic conditions. Compound **9h** displays less hypoxia selectivity than tirapazamine. Hypoxia-selective cytotoxicity is quantitatively defined by the hypoxic cytotoxicity ratio (HCR). In the present work, we define HCR as the ratio of doses required to give 99% cell kill under aerobic versus hypoxic conditions. We found that the HCR for **9h** was 16 whereas that measured for tirapazamine previously using the same conditions was 75.<sup>44,45</sup>

### 2.5. Comparison of redox-cycling by **9h** and tirapazamine

It is well established that one-electron reduction of tirapazamine under aerobic conditions results in redox cycling reactions that yield superoxide radical (left side, Scheme 1).<sup>6,8,9,12,13,19–23</sup> We recently provided evidence that **9h** undergoes similar enzyme-driven redox cycling under aerobic conditions.<sup>43</sup> With the goal of gaining deeper insight into the molecular origins of the different HCRs displayed by **9h** and tirapazamine, we conducted a side-by-side comparison of the redox-cycling properties of **9h** and tirapazamine. We employed the plasmid-based DNA-cleavage assay described above for the quantitative detection of superoxide radical generation in these experiments. The plasmid assay previously has been used to detect superoxide generation.<sup>77–81</sup> In the current assays, the di-N-oxides were incubated under aerobic conditions in the presence of the NADPH:cytochrome P450 reductase enzyme system. In contrast to the anaerobic assays described above, the reaction mixtures in these aerobic experiments did not contain SOD, catalase, or metal chelators that would squelch strand cleavage stemming from superoxide radical. Previous work has shown that DNA cleavage under these (aerobic) conditions does not stem from release of N-oxide oxygens as hydroxyl radical.<sup>6,8,9,12,13,19–23</sup> Rather, under these conditions, superoxide radical generated by redox cycling leads to DNA strand cleavage via the cascade of reactions shown in (unbalanced) Eq. 1.<sup>6,71</sup>



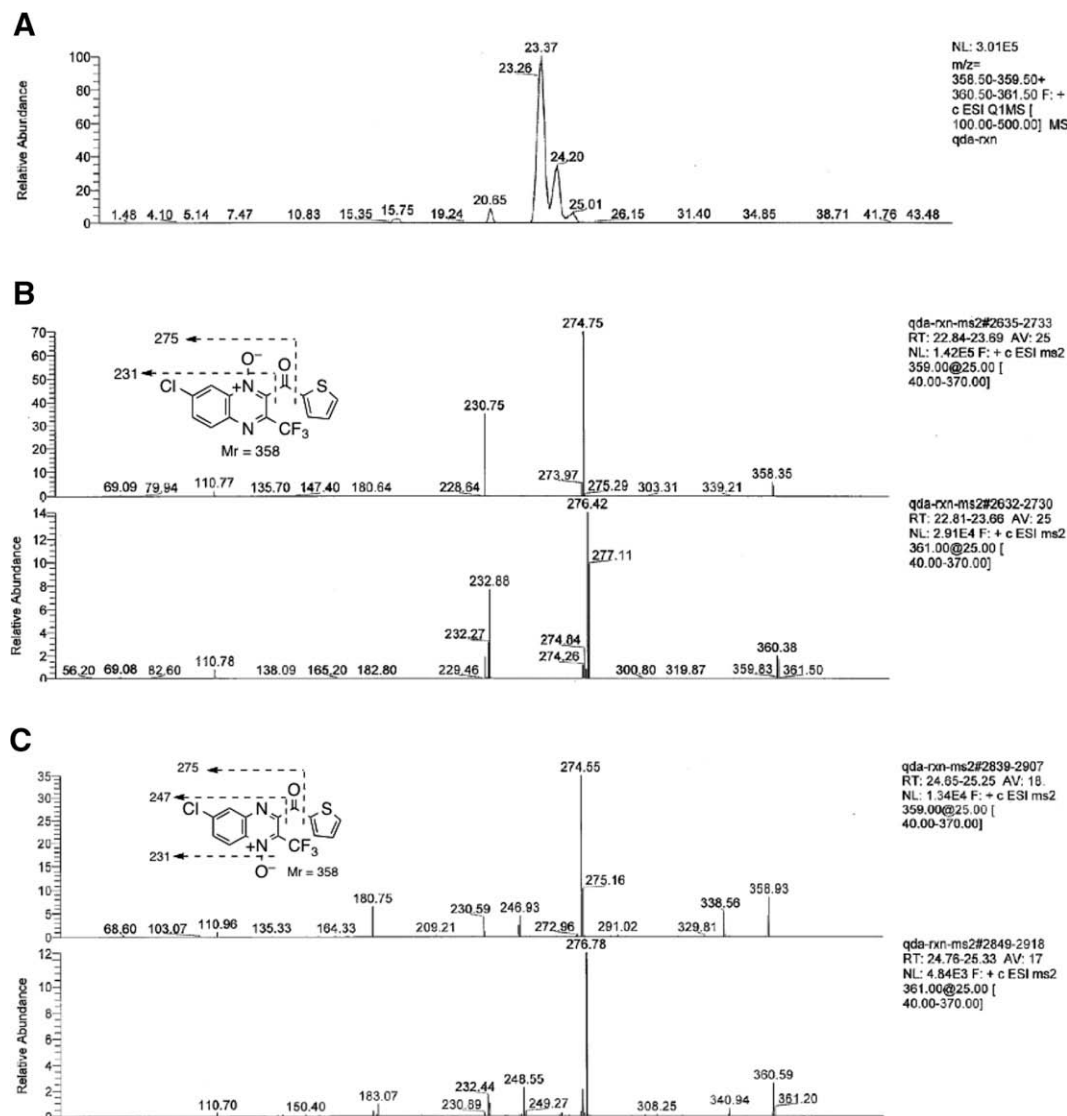
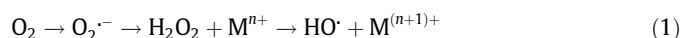
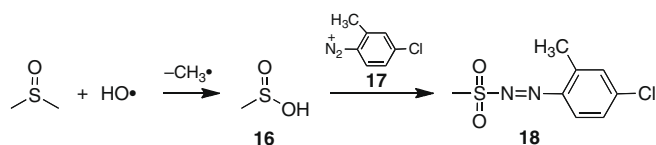


**Figure 6.** LC/MS analysis of the products generated by in vitro metabolism of 9h by NADPH:cytochrome P450 reductase under anaerobic conditions. Compound 9h (200  $\mu$ M) was incubated with NADPH:cytochrome P450 reductase (330 mU/mL) and NADPH (500  $\mu$ M) in sodium phosphate buffer (pH 7.0, 50 mM), acetonitrile (20% v/v) containing desferal (1 mM) for 16 h, under anaerobic conditions. The resulting mixture was analyzed by LC/MS and LC/MS/MS as described in Section 4. Panel A: selected-ion chromatogram monitoring the ions corresponding to the  $[M+H]^+$  and  $[M+2+H]^+$  isotopomers of the anticipated mono-N-oxide metabolites 12 and 13 ( $m/z$  360 and 361). Panel B: LC/MS/MS analysis of the  $m/z$  358 and 360  $[M+H]^+$  ions generated by metabolite eluting at 23 min in the chromatogram shown in panel A. Panel C: LC/MS/MS analysis of the  $m/z$  358 and 360  $[M+H]^+$  ions generated by the metabolite eluting at 25 min in the chromatogram shown in panel A.



As reported previously,<sup>43</sup> incubation of **9h** (25  $\mu$ M) with NADPH:cytochrome P450 reductase (33 mU/mL), NADPH (500  $\mu$ M), in sodium phosphate buffer (50 mM, pH 7.0) containing 2.5% acetonitrile (v/v) under aerobic conditions at 24  $^{\circ}$ C for 2 h leads to strand cleavage that is comparable to the archetypal redox-cycling agent menadione (Fig. 7).<sup>6,71</sup> However, strand cleavage by tirapazamine under these conditions is less than half of that caused by **9h**. The reasons for the comparatively weak redox

cycling activity of tirapazamine are not clear at this time. Nonetheless, the results suggest that superior redox cycling capabilities could contribute to the greater aerobic toxicity of **9h**.

### 3. Conclusion

Compound **9h** displays hypoxia-selective, enzyme-activated DNA-cleaving properties similar to drug candidate tirapazamine. This provides further evidence that structurally varied heterocyclic N-oxides can recapitulate the medically interesting properties associated with tirapazamine. While the DNA-cleaving activity of **9h** closely parallels that of tirapazamine, there are some interesting differences in the bioactivities of these two compounds. Compound **9h** displays a HCR of 16 against V79 Chinese hamster lung fibroblasts, whereas tirapazamine is substantially more hypoxia selective, with an HCR of 75.<sup>44,45</sup> Superior redox cycling properties of **9h** may contribute to its greater aerobic toxicity. It is noteworthy that **9h** is more cytotoxic than tirapazamine under both

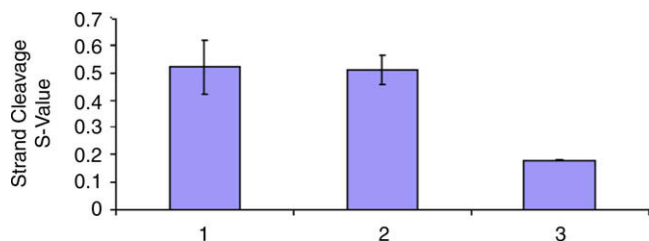


**Figure 7.** Comparison of DNA-cleavage by **9h**, menadione, and tirapazamine (**1**) in the presence of NADPH:cytochrome P450 reductase under aerobic conditions. Reactions containing supercoiled plasmid DNA (33 µg/mL, pGL-2 Basic) were incubated with **9h** (bar 1) or menadione (bar 2) or **1** (bar 3) (25 µM), NADPH (500 µM) and cytochrome P450 reductase (33 mU/mL) in sodium phosphate buffer (50 mM, pH 7), acetonitrile (2.5% v/v) under aerobic conditions at room temperature for 2 h, followed by agarose gel electrophoretic analysis. The values, strand breaks per plasmid (*S*), derived from agarose gel data and represent the mean number of strand breaks per plasmid molecule and were calculated using the equation  $S = -\ln f_i$ , where  $f_i$  is the fraction of plasmid present as form I. Background cleavage in the untreated plasmid was subtracted to allow direct comparison of DNA cleavage yields between different experiments.

hypoxic and aerobic conditions, giving 99% cell kill at 2.5 µM and 0.21 µM under aerobic and anaerobic conditions, respectively. Tirapazamine gives 99% cell kill at 30 µM and 2.0 µM under aerobic and anaerobic conditions, respectively. The reasons for the higher general potency of **9h** as compared to tirapazamine remain uncertain. It is tempting to suggest that the thienyl group contributes to the potent cell-killing properties of **9h** because thienyl groups are known to generate cytotoxic metabolites.<sup>82,83</sup> However, this explanation is not completely satisfying because other analogues in this series bearing aryl or naphthyl substituents at this position show cytotoxicity against various cancer cell lines that is comparable to the thienyl derivative **9h** (although it is interesting to note that the aryl compounds do not display activity comparable to **9h** in the hollow fiber assay).<sup>43</sup>

Finally, it may be useful to consider the potential medicinal relevance of the differences between **9h** and tirapazamine. Along these lines it is important to point out that despite more than 20 years of study and multiple clinical trials, tirapazamine has not yet found a clinically approved application. Indeed, it seems likely that success within this class of compounds may depend upon the development of new heterocyclic N-oxides whose properties differ from tirapazamine.<sup>40</sup> In this light, the lower HCR and higher cytotoxicity of **9h** relative to tirapazamine may not necessarily be drawbacks. In fact, recent reviews have suggested that the failure of tirapazamine to perform in the clinical setting may be due to its relatively low toxicity as a sole agent or the fact that not all tumors contain severely hypoxic regions.<sup>33</sup> Compound **9h** is both more cytotoxic and less hypoxia selective than tirapazamine. With these ideas in mind, further preclinical evaluation of **9h** and related compounds is underway.

## 4. Experimental

### 4.1. General

Materials were of the highest purity available and were obtained from following sources: sodium phosphate, mannitol, xanthine, and DMSO from Aldrich Chemical Co. (Milwaukee, WI); NADPH, desferal, cytochrome P450 reductase, catalase, and superoxide dismutase (SOD) from Sigma Chemical Co. (St. Louis, MO); xylene cyanol, bromophenol blue, and formamide, from United States Biochemical; xanthine oxidase from Roche Diagnostics; agarose from Seakem; HPLC grade solvents (acetonitrile, methanol, ethanol, *tert*-butyl alcohol, ethyl acetate, hexane, and acetic acid) from Fischer (Pittsburgh, PA); ethidium bromide from Roche

Molecular Biochemicals (Indianapolis, IN). The plasmid pGL2BASIC was prepared using standard protocols.<sup>55</sup> Tirapazamine (**1**) and other N-oxides were synthesized according to literature methods.<sup>43,56</sup>

### 4.2. Anaerobic DNA cleavage assays

Supercoiled plasmid DNA (33 µg/mL, pGL-2 Basic) was incubated with tirapazamine or **9h** (5–25 µM), NADPH (500 µM), cytochrome P450 reductase (33 mU/mL), catalase (100 µg/mL), superoxide dismutase (10 µg/mL), sodium phosphate buffer (50 mM, pH 7.0), acetonitrile (0.5–2.5% v/v), and desferal (1 mM) under anaerobic conditions at 25 °C for 16 h. All components of the reactions except enzymes, NADPH, and DNA were deoxygenated by three freeze-pump-thaw cycles. Enzymes, NADPH, and DNA were diluted with deoxygenated water in an argon-filled glove bag to prepare stock solutions. Reactions were initiated by adding cytochrome P450 reductase, wrapped in aluminum foil to prevent exposure to light, and incubated in an argon filled glove bag. Following incubation, the reactions were quenched by addition of 5 µL of 50% glycerol loading buffer<sup>55</sup> and were loaded onto a 0.9% agarose gel. The gel was electrophoresed for approximately 2.5 h at 82 V in 1 × TAE buffer before staining in a solution of aqueous ethidium bromide (0.3 µg/mL) for 3 h. DNA in the gel was visualized by UV-transillumination, and the amount of DNA in each band was quantified using an Alpha Innotech IS-1000 digital imaging system. The values reported are not corrected for differential staining of form I and form II DNA by ethidium bromide.<sup>57</sup> DNA cleavage assays containing radical scavengers were carried out as described above except radical scavengers such as methanol, ethanol, *tert*-butyl alcohol, DMSO, or mannitol (500 mM) were added before initiating reactions with the cytochrome P450 reductase. Aerobic control reactions were carried out similar to anaerobic assays except reaction components were not degassed and the assays were incubated under ambient conditions.

### 4.3. In vitro anaerobic metabolism of **9h**

A solution containing **9h** (200 µM in 20% acetonitrile/water v/v) and desferal (1 mM) in sodium phosphate buffer (pH 7, 50 mM) was deoxygenated by three cycles of freeze-pump-thaw degassing. The degassed solution was transferred to microcentrifuge tube in an argon filled glove bag. To this mixture, NADPH (500 µM), cytochrome P450 reductase (330 mU/mL), catalase (100 µg/mL), and superoxide dismutase (10 µg/mL) were added and the mixture incubated under argon at 25 °C for 16 h. An otherwise identical control reaction with **9h** in the absence of enzyme was carried out. Enzymes and NADPH were diluted with deoxygenated water. Prior to analysis by HPLC, proteins were removed from the reaction mixture by centrifugation through Amicon Microcon (YM3) filters. The filtrate was analyzed by HPLC employing a C18 reverse phase Rainin Microsorb-MV column (5 µm particle size, 100 Å pore size, 25 cm length, 4.6 mm i.d.) eluted with gradient starting at 50% A (0.5% acetic acid in water) and 50% B (acetonitrile) followed by linear increase to 80% B from 0 min to 40 min. A flow rate of 0.6 mL/min was used and the products were monitored by their UV-absorbance at 254 nm. In vitro metabolism of **9h** by NADPH:cytochrome P450 reductase yields three products. The relative yields of these products appears similar when judged by UV-vis or ion current in the LC/ESI-MS. The major product eluting at 23 min co-elutes with an authentic samples of 1-N-oxide, while the minor product eluting at 25 min co-elutes with an authentic sample of the 4-N-oxide. Prior to LC/MS analysis, metabolites were extracted into ethyl acetate and dried, and redissolved in 50:50 acetonitrile/water. LC/ESI-MS experiments were carried out on a Finnigan TSQ 7000 triple quadrupole instrument interfaced to a ThermoSep-

arations liquid chromatograph (TSP4000). Positive ion electrospray was used as the means of ionization. The heated inlet capillary temperature was 250 °C and electrospray needle voltage was 4.5 kV. Nitrogen sheath gas was supplied at 80 psi. Analysis by LC/ESI-MS in the positive ion mode confirmed that these products have masses consistent with mono-N-oxide metabolites.

#### 4.4. Oxidation of DMSO to methanesulfinic acid by enzymatically-activated **9h**

Methanesulfinic acid produced by the oxidation of DMSO during in vitro metabolism of **9h** was quantitatively measured using a modified version of the protocol reported by Fukui et al.<sup>58</sup> In a typical assay, individual components of the reactions were deoxygenated as described above. To a degassed solution containing sodium phosphate (50 mM, pH 7.0), **9h** (300 µM) and desferal (1 mM), deoxygenated DMSO (2.5 M), NADPH (1 mM) and cytochrome P450 reductase (0.146 U/mL) were added. The reaction (1 mL final volume) was capped, mixed, and allowed to incubate under an argon atmosphere at 24 °C for 4 h. Then a solution of sodium phosphate (0.5 mL, 500 mM, pH 4.0) was added to the reaction, followed by Fast Red TR diazonium salt (**14**, 0.5 mL of a 10 mg/mL solution in water) and the mixture was then allowed to stand at room temperature for 10 min. During this time an orange color developed. The resulting solution was then extracted with ethyl acetate (2 × 1 mL) and exactly 1.2 mL of the ethyl acetate layer removed by pipette. A portion of this ethyl acetate solution (20 µL) containing the methane diazosulfone **18** was analyzed by HPLC. The diazosulfone conjugate **18** was observed by its absorbance at 310 nm at a retention time of approximately 9 min on a Rainin Microsorb-MV propylamine column eluted with hexane/2-propanol (100:3 v/v) at a flow rate of 1 mL/min. Authentic **18** for comparison was prepared as previously described.<sup>21,58</sup> For the construction of calibration curves, known amounts of methanesulfinic acid were dissolved in sodium phosphate buffer (50 mM, pH 7.0) to make 1 mL solutions containing different concentrations of methane sulfinic acid (100–500 µM). To these solutions, sodium phosphate buffer (0.5 mL, 500 mM, pH 4.0) was added, followed by Fast Red TR diazonium salt (**17**, 0.5 mL of 10 mg/mL). The reactions were allowed to stand at room temperature for 10 min and the resulting orange solutions extracted with ethyl acetate (2 × 1 mL) and exactly 1.2 mL of the upper ethyl acetate layer removed by pipette. A portion of this ethyl acetate solution (20 µL) containing the methane diazosulfone was then analyzed and quantified by HPLC. Injection-to-injection variation in this system is less than 5%. Control reactions containing **9h** but lacking either NADPH or enzyme were performed. The final reported yields of **18** were corrected for the low background levels methanesulfinic acid measured in these control reactions and for unmetabolized di-N-oxide.

#### 4.5. Aerobic and hypoxic cytotoxicity toward V79 cells

V79 cells (Chinese hamster lung fibroblasts) were obtained from ECACC (European Collection of Animal Cell Cultures) and maintained in logarithmic growth as subconfluent monolayers by trypsinization and subculture to (1–2) × 10<sup>4</sup> cells/cm<sup>2</sup> twice weekly. The growth medium was EMEM (Eagle's minimal essential medium), containing 10% (v/v) fetal bovine serum (FBS) and penicillin/streptomycin at 100 U/100 µg/mL. Monolayers of V79 cells in exponential growth were trypsinized, and suspension cultures were set up in 50 mL glass flasks: 2 × 10<sup>4</sup> cells/mL in 30 mL of EMEM containing 10% (v/v) FBS and HEPES (10 mM). The glass flasks were submerged and stirred in a water bath at 37 °C, where they were gassed with humidified air or pure nitrogen. Compounds solutions were prepared just before dosing. Stock solutions, 150-fold more concentrated, were prepared in pure DMSO (Aldrich).

Thirty minutes after the start of gassing, 0.2 mL of the stock compound solution was added to each flask, two flasks per dose. In every assay there was one flask with 0.2 mL of DMSO (negative control). After 2 h exposure to the compound, the cells were centrifuged and resuspended in plating medium (EMEM plus 10% (v/v) FBS and penicillin/streptomycin). Cell numbers were determined with a haemocytometer and 10<sup>2</sup>–10<sup>3</sup> cells were plated in 6-well (30 mm diameter) plates to give a final volume of 2 mL per well. Plates were incubated at 37 °C in 5% CO<sub>2</sub> for seven days and then stained with aqueous crystal violet. Colonies with more than 64 cells were counted. The plating efficiency (PE) was calculated by dividing the number of colonies by the number of cells seeded. The Survival Percentage (SP) of treated cells with respect to the control was calculated by the following formula = PE of treated cells/PE of control cells × 100. The selectivity of the compounds was determined by the hypoxic cytotoxicity ratio (HCR) = concentration in normoxia/concentration in hypoxia giving 1% of SP.

#### 4.6. Comparison of aerobic redox cycling by **9h**, menadione, and tirapazamine

In a typical reaction, supercoiled plasmid DNA (33 µg/mL, pGL-2 Basic), **9h**, tirapazamine, or menadione (25 µM), NADPH (500 µM) and NADPH:cytochrome P450 reductase (1 mU) were incubated in sodium phosphate buffer (50 mM, pH 7.0) containing 2.5% acetonitrile under aerobic conditions at 24 °C for 2 h. Compound **9h** and menadione were introduced as stock solutions in acetonitrile. Following incubation, the reactions were stopped by addition of 50% glycerol loading buffer (5 µL), and the resulting mixture loaded onto a 0.9% agarose gel. The topological forms of plasmid DNA were separated by electrophoresis at 85 V in 1 × TAE buffer and then stained by immersing the gel in a solution of aqueous ethidium bromide (0.3 µg/mL) for 2 h. DNA in the gel was visualized by UV-transillumination, and the amount of DNA in each band was quantified using an Alpha Innotech IS-1000 digital imaging system.

#### Acknowledgments

The authors are grateful to the National Institutes of Health (CA 100757 to K.S.G.) for partial financial support of this work. This work has received financial support from the Government of Navarra within the program of the Work Community of Pyrenees. Project CTP 07/P11 and Fondo de Investigaciones Sanitarias (PPT-090000-2008-4).

#### References and notes

- Bertout, J. A.; Patel, S. A.; Simon, M. C. *Nat. Rev. Cancer* **2008**, *8*, 967.
- Vaupel, P. *Oncologist* **2008**, *13*, 21.
- Dachs, G. U.; Stratford, I. J. *Br. J. Cancer* **1996**, *74*, S126.
- Brown, J. M.; Wilson, W. R. *Nat. Rev. Cancer* **2004**, *4*, 437.
- Denny, W. A. *Lancet Oncol.* **2000**, *1*, 25.
- Wardman, P. *Curr. Med. Chem.* **2001**, *8*, 739.
- Chen, Y.; Hu, L. *Med. Res. Rev.* **2009**, *29*, 29.
- Wardman, P.; Priyadarsini, K. I.; Dennis, M. F.; Everett, S. A.; Naylor, M. A.; Patel, K. B.; Stratford, I. J.; Stratford, M. R. L.; Tracy, M. *Br. J. Cancer* **1996**, *74*, S70.
- Brown, J. M. *Br. J. Cancer* **1993**, *67*, 1163.
- Kelson, A. B.; McNamara, J. P.; Pandey, A.; Ryan, K. J.; Dorie, M. J.; McAfee, P. A.; Menke, D. R.; Brown, J. M.; Tracy, M. *Anti-Cancer Drug. Des.* **1998**, *13*, 575.
- Cerretto, H.; González, M. *Mini-Rev. Med. Chem.* **2001**, *1*, 219.
- Baker, M. A.; Zeman, E. M.; Hirst, V. K.; Brown, J. M. *Cancer Res.* **1988**, *48*, 5947.
- Biedermann, K. A.; Wang, J.; Graham, R. P. *Br. J. Cancer* **1991**, *63*, 358.
- Wang, J.; Biedermann, K. A.; Brown, J. M. *Cancer Res.* **1992**, *52*, 4473.
- Peters, K. B.; Tung, J. J.; Brown, J. M. *Cancer Res.* **2002**, *62*, 5248.
- Daniels, J. S.; Gates, K. S.; Tronche, C.; Greenberg, M. M. *Chem. Res. Toxicol.* **1998**, *11*, 1254.
- Hwang, J.-T.; Greenberg, M. M.; Fuchs, T.; Gates, K. S. *Biochemistry* **1999**, *38*, 14248.
- Kotandeniya, D.; Ganley, B.; Gates, K. S. *Bioorg. Med. Chem. Lett.* **2002**, *12*, 2325.
- Laderoute, K. L.; Wardman, P.; Rauth, M. *Biochem. Pharmacol.* **1988**, *37*, 1487.

20. Fitzsimmons, S. A.; Lewis, A. D.; Riley, R. J.; Workman, P. *Carcinogenesis* **1994**, 15, 1503.
21. Daniels, J. S.; Gates, K. S. *J. Am. Chem. Soc.* **1996**, 118, 3380.
22. Costa, A. K.; Baker, M. A.; Brown, J. M.; Trudell, J. R. *Cancer Res.* **1989**, 49, 925.
23. Priyadarsini, K. I.; Tracy, M.; Wardman, P. *Free Radical Res.* **1996**, 25, 393.
24. Junnotula, V.; Sarkar, U.; Sinha, S.; Gates, K. S. *J. Am. Chem. Soc.* **2009**, 131, 1015.
25. Chowdhury, G.; Junnotula, V.; Daniels, J. S.; Greenberg, M. M.; Gates, K. S. *J. Am. Chem. Soc.* **2007**, 129, 12870.
26. Birincioglu, M.; Jaruga, P.; Chowdhury, G.; Rodriguez, H.; Dizdaroglu, M.; Gates, K. S. *J. Am. Chem. Soc.* **2003**, 125, 11607.
27. Li, L.-C.; Zha, D.; Zhu, Y.-Q.; Xu, M.-H.; Wong, N.-B. *Chem. Phys. Lett.* **2005**, 408, 329.
28. Shinde, S. S.; Anderson, R. F.; Hay, M. P.; Gamage, S. A.; Denny, W. A. *J. Am. Chem. Soc.* **2004**, 126, 7865.
29. Shinde, S. S.; Hay, M. P.; Patterson, A. V.; Denny, W. A.; Anderson, R. F. *J. Am. Chem. Soc.* **2009**, 131, 14220.
30. Anderson, R. F.; Shinde, S. S.; Hay, M. P.; Gamage, S. A.; Denny, W. A. *J. Am. Chem. Soc.* **2003**, 125, 748.
31. Anderson, R. F.; Shinde, S. S.; Hay, M. P.; Gamage, S. A.; Denny, W. A. *Org. Biomol. Chem.* **2005**, 3, 2167.
32. Gandara, D. R.; Lara, P. N.; Goldberg, Z.; Le, Q. T.; Mack, P. C.; Lau, D. H. M.; Gumerlock, P. H. *Sem. Oncol.* **2002**, 29, 102.
33. Marcu, L.; Olver, I. *Curr. Clin. Oncol.* **2006**, 1, 71.
34. Jiang, F.; Weng, Q.; Sheng, R.; Xia, Q.; He, Q.; Yang, B.; Hu, Y. *Arch. Pharm. Chem. Life Sci.* **2007**, 340, 258.
35. Hay, M. P.; Gamage, S. A.; Kovacs, M. S.; Pruijn, F. B.; Anderson, R. F.; Patterson, A. V.; Wilson, W. R.; Brown, J. M.; Denny, W. A. *J. Med. Chem.* **2003**, 46, 169.
36. Hay, M. P.; Hicks, K. O.; Pruijn, F. B.; Pchalek, K.; Siim, B. G.; Wilson, W. R.; Denny, W. A. *J. Med. Chem.* **2007**, 50, 6392.
37. Hay, M. P.; Pchalek, K.; Pruijn, F. B.; Hicks, K. O.; Siim, B. G.; Anderson, M. M.; Shinde, S. S.; Denny, W. A.; Wilson, W. R. *J. Med. Chem.* **2007**, 50, 6654.
38. Hay, M. P.; Pruijn, F. B.; Gamage, S. A.; Liyanage, H. D. S.; Kovacs, M. S.; Patterson, A. V.; Wilson, W. R.; Brown, J. M.; Denny, W. A. *J. Med. Chem.* **2004**, 47, 475.
39. Hay, M. P.; Denny, W. A. *Tetrahedron Lett.* **2002**, 43, 9569.
40. Hay, M. P.; Hicks, K. O.; Pchalek, K.; Lee, H. H.; Blaser, A.; Pruijn, F. B.; Anderson, R. F.; Shinde, S. S.; Wilson, W. R.; Denny, W. A. *J. Med. Chem.* **2008**, 51, 6853.
41. Chowdhury, G.; Kotandeniya, D.; Barnes, C. L.; Gates, K. S. *Chem. Res. Toxicol.* **2004**, 17, 1399.
42. Ganley, B.; Chowdhury, G.; Bhansali, J.; Daniels, J. S.; Gates, K. S. *Bioorg. Med. Chem.* **2001**, 9, 2395.
43. Solano, B.; Junnotula, V.; Marin, A.; Villar, R.; Burguete, A.; Vicente, E.; Perez-Silanes, S.; Monge, A.; Dutta, S.; Sarkar, U.; Gates, K. S. *J. Med. Chem.* **2007**, 50, 5485.
44. Monge, A.; Martinez-Crespo, F. J.; Lopez de Cerain, A.; Palop, J. A.; Narro, S.; Senador, V.; Marin, A.; Sainz, Y.; Gonzalez, M.; Hamilton, E.; Barker, A. J.; Clarke, E. D.; Greenhow, D. T. *J. Med. Chem.* **1995**, 38, 4488.
45. Monge, A.; Palop, J. A.; de Cerain, A. L.; Senador, V.; Martinez-Crespo, F. J.; Sainz, Y.; Narro, S.; Garcia, E.; de Miguel, C.; Gonzalez, M.; Hamilton, E.; Barker, A. J.; Clarke, E. D.; Greenhow, D. T. *J. Med. Chem.* **1995**, 38, 1786.
46. Monge, A.; Palop, J. A.; Pinol, A.; Martinez-Crespo, F. J.; Narro, S.; Gonzalez, M.; Sainz, Y.; Lopez de Cerain, A.; Hamilton, E.; Barker, A. J. *J. Heterocycl. Chem.* **1994**, 31, 1135.
47. Gonzalez, M.; Cerecetto, H.; Monge, A. *Topics Heterocycl. Chem.* **2007**, 11, 179.
48. Cerecetto, H.; Gonzalez, M.; Lavaggi, M. L.; Azqueta, A.; de Cerain, A. L.; Monge, A. *J. Med. Chem.* **2005**, 48, 21.
49. Lavaggi, M. L.; Cabrera, M.; González, M.; Cerecetto, H. *Chem. Res. Toxicol.* **2008**, 21, 1900.
50. Nagai, K.; Carter, B. J.; Xu, J.; Hecht, S. M. *J. Am. Chem. Soc.* **1991**, 113, 5099.
51. Nagai, K.; Hecht, S. M. *J. Biol. Chem.* **1991**, 266, 23994.
52. Priyadarsini, K. I.; Dennis, M. F.; Naylor, M. A.; Stratford, M. R. L.; Wardman, P. *J. Am. Chem. Soc.* **1996**, 118, 5648.
53. Klinkenberg, L. G.; Sutherland, L. A.; Bishai, W. R.; Karakousis, P. C. *J. Infect. Dis.* **2008**, 198, 275.
54. Sullivan, J. P.; Palmer, A. F. *Biotechnol. Prog.* **2006**, 22, 1374.
55. Sambrook, J.; Fritsch, E. F.; Maniatis, T. *Molecular Cloning: A Lab Manual*; Cold Spring Harbor Press: Cold Spring Harbor, NY, 1989.
56. Fuchs, T.; Chowdhary, G.; Barnes, C. L.; Gates, K. S. *J. Org. Chem.* **2001**, 66, 107.
57. Bauer, W.; Vinograd, J. *J. Mol. Biol.* **1968**, 33, 141.
58. Fukui, S.; Hanasaki, Y.; Ogawa, S. *J. Chromatogr.* **1993**, 630, 187.
59. Patterson, A. V.; Saunders, M. P.; Chinje, E. C.; Patterson, L. H.; Stratford, I. J. *Anti-Cancer Drug Des.* **1998**, 13, 541.
60. Walton, M. I.; Wolf, C. R.; Workman, P. *Biochem. Pharmacol.* **1992**, 44, 251.
61. Hintermann, G.; Fischer, H. M.; Cramer, R.; Hutter, R. *Plasmid* **1981**, 5, 371.
62. Jonson, P. H.; Grossman, L. I. *Biochemistry* **1977**, 16, 4217.
63. Mirabelli, C. K.; Huang, C. H.; Fenwick, R. G.; Crooke, S. T. *Antimicrobial Agents Chemother.* **1985**, 27, 460.
64. Greenberg, M. M. *Org. Biomol. Chem.* **2007**, 5, 18.
65. Greenberg, M. M. *Chem. Res. Toxicol.* **1998**, 11, 1235.
66. Pogozelski, W. K.; Tullius, T. D. *Chem. Rev.* **1998**, 98, 1089.
67. Breen, A. P.; Murphy, J. A. *Free Radical Biol. Med.* **1995**, 18, 1033.
68. Prati, G.; Bernadou, J.; Meunier, B. *Angew. Chem., Int. Ed. Engl.* **1995**, 34, 746.
69. Gates, K. S. Chemical reactions of DNA Damage and Degradation. In *Reviews of Reactive Intermediates*; Platz, M. S. M. R. A., Jones, M., Jr., Eds.; John Wiley and Sons, Inc.: Hoboken, 2007; pp 333–378.
70. Gates, K. S. *Chem. Res. Toxicol.* **2009**, 22, 1747.
71. Halliwell, B.; Gutteridge, J. M. C. *Methods Enzymol.* **1990**, 186, 1.
72. Laderoute, K.; Rauth, A. M. *Biochem. Pharmacol.* **1986**, 35, 3417.
73. Zeman, E. M.; Brown, J. M.; Lemmon, M. J.; Hirst, V. K.; Lee, W. W. *Int. J. Radiat. Oncol. Biol. Phys.* **1986**, 12, 1239.
74. Steiner, M. G.; Babbs, C. F. *Arch. Biochem. Biophys.* **1990**, 278, 478.
75. Klein, S. M.; Cohen, G.; Cederbaum, A. I. *Biochemistry* **1981**, 20, 6006.
76. Babbs, C.; Steiner, M. G. *Methods Enzymol.* **1990**, 186, 137.
77. Chatterji, T.; Gates, K. S. *Bioorg. Med. Chem. Lett.* **1998**, 8, 535.
78. Chatterji, T.; Gates, K. S. *Bioorg. Med. Chem. Lett.* **2003**, 13, 1349.
79. Chatterji, T.; Keerthi, K.; Gates, K. S. *Bioorg. Med. Chem. Lett.* **2005**, 15, 3921.
80. Kim, W.; Dannaldson, J.; Gates, K. S. *Tetrahedron Lett.* **1996**, 37, 5337.
81. Mitra, K.; Gates, K. S. *Recent Res. Dev. Org. Chem.* **1999**, 3, 311.
82. López-García, M. P.; Dansette, P. M.; Mansuy, D. *Biochemistry* **1994**, 33, 166.
83. Lash, L. H.; Tokarz, J. J. *Toxicology* **1995**, 103, 167.